Twelfth Australasian Fluid Mechanics Conference
The University of Sydney, Australia 1995

ROTATING STALL IN MIXED-FLOW TURBOMACHINES

A.Yadoiwa[1], N.Ito[1], S.Akaike[2], A.Whitfield[3], T.Sakai[1]
[1]Science University of Tokyo
1-3, Kagurazaka, Shinjuku-ku, Tokyo 162 JAPAN
[2]Kanagawa Institute of Technology
1030 Shimo-ogino, Atsugi 243-02 JAPAN
[3]University of Bath
Claverton Down, Bath BA2 7AY U.K.

Abstract

The development of rotating stall in the mixed-flow turbomachines which combine two types of impellers and two types of mixed-flow diffusers was studied experimentally. Rotating stall was detected in the impeller and the diffuser. The inception of the impeller rotating stall was effected by flow reversals on the shroud side of the impeller inlet and on hub side in the diffuser. From the observation of flow visualization tufts and measurement of the internal flow, the dependence of rotating stall on the diffuser design and impeller blade number was clarified.

Nomenclature

b depth of flow passage (m)
u tip speed of impeller (m/s)
R radius (m)
α cone angle (deg)
Q volume flow rate (m^3/min)
H total head
between inlet and exit of impeller (m)
N rotational speed of impeller (rpm)
N_s specific speed ($= N\sqrt{Q} / H^{3/4}$)
C_m meridional component of velocity (m/s)
ϕ flow coefficient ($=C_{m2}/u_2$)
ψ pressure coefficient ($=gH/u_2^2$)
β impeller angle from the tangential direction (deg)
θ impeller inlet flow angle
from the tangential direction (deg)

Subscripts

1 impeller inlet
2 impeller exit
3 diffuser exit

Introduction

The internal flow of the mixed-flow turbomachine behaves differently from that of the centrifugal machine due to the pressure gradient normal to the flow passage generated by the centrifugal force of the swirling flow. Consequently unstable flow is more likely to develop in the mixed-flow machine than in the centrifugal machine. This was shown by Abir and Whitfield (1987) by testing a pure conical diffuser and a number of curved annular diffusers. Their tests were conducted on a large scale model of a mixed flow compressor and used a rotating screen to generate the diffuser inlet swirling flow rather than an impeller. They showed the inherent instability of the pure conical diffuser but did not report the effect of rotating stall; their experimental facility did not permit a study of the development of flow pulsations through the impeller. In this study the behaviour of rotating stall in mixed flow turbomachines, with six and twelve bladed impellers, has been examined with both pure conical(PC) and curved annular(CA) vaneless diffusers, see Fig.1. From time dependent flow measurements at the impeller inlet and in the diffuser passage, rotating stall caused by impeller and diffuser stall was captured. Time averaged flow traverse measurements with a three hole cobra type Pitot probe were also made to determine mean internal flow as the rotating stall developed. To confirm the rotating stall in the impeller and diffuser, flow visualization studies were made at impeller inlet and in the diffuser passage by the use of fine tufts made of nylon cord and dandelion pappus attached to the rotating blade suction surface and diffuser walls. The response of this tuft for up to 400 Hz flow fluctuation was confirmed by Sakai et al (1994) in the Karman vortex street using high speed video system. Through these experiments the relationship between the diffuser flow and impeller rotating stall was clarified. It was also found that the machine with 6 impeller blades caused less severe stall.

Apparatus and Instrumentation

The experimental test facilities are shown in Fig.1. For this investigation a mixed-flow blower with a specific speed of N_s=500 (rpm,m,m^3/min) was used together with two alternative vaneless diffuser designs. For the purpose

of flow visualization, the walls of the diffuser and the impeller inlet duct were made of Plexiglas. The specification of the impeller and the diffuser was as follows:

Cone angle of impeller exit α_2 120 deg
Mean radius of impeller exit R_2 0.1 m
Impeller inlet blade angle β_1 40 deg
Impeller exit blade angle β_2 60 deg
Mean radius of diffuser exit R_3 0.25 m
Depth of diffuser passage $b_2=b_3$ 0.026 m (constant)
Radius of curvature at the mean line of curved part R_s 0.03 m (CA)

Pressure transducers were used to detect pressure pulsations at impeller inlet and at two stations 90° apart in the diffuser. Velocity fluctuations were measured with a hot wire anemometer. Photography of fine tufts both in the diffuser and, with the aid of a stroboscopic lamp within the impeller inlet passage was used to visualize the flow. The exposure time of the pictures was 1 second. Mean flow conditions at impeller inlet and discharge into the diffuser were measured with a three hole cobra probe which was made from 0.7mm stainless steel tubes. The maximum projected area of this probe was approximately 0.3 percent of the passage flow area and the influence of the probe on the flow field was considered to be small. The head of the flow visualization tufts was made of dandelion pappus and attached to the surface with 0.35mm nylon cord; this was trimmed short to ensure that the characteristics of the flow close to the wall surface could be observed.

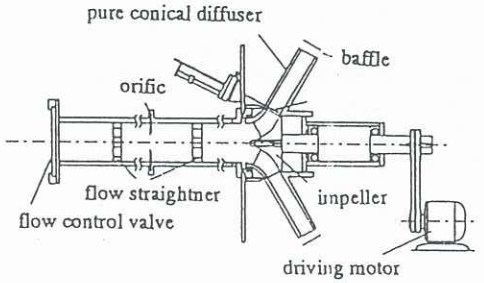

PC type arrangement

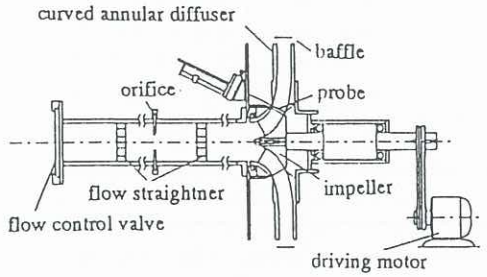

CA type arrangement

Fig.1 :Experimental arrangement

Results

The basic performance of the 12 bladed impeller with both diffuser designs is shown in Fig.2 in terms of the variation of pressure coefficient with flow coefficient; the corresponding performance for the 6 bladed impeller is

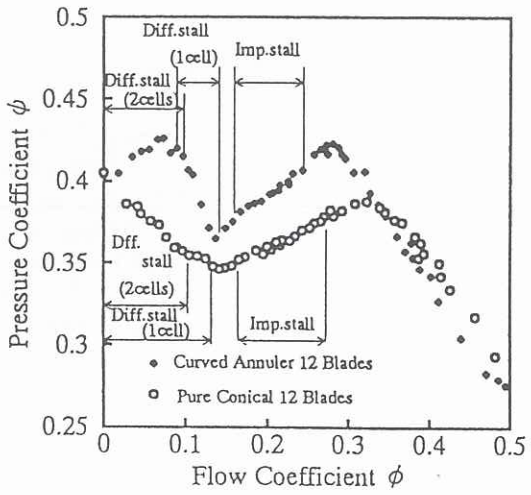

Fig.2 :Pressure coefficient vs. Flow coefficient

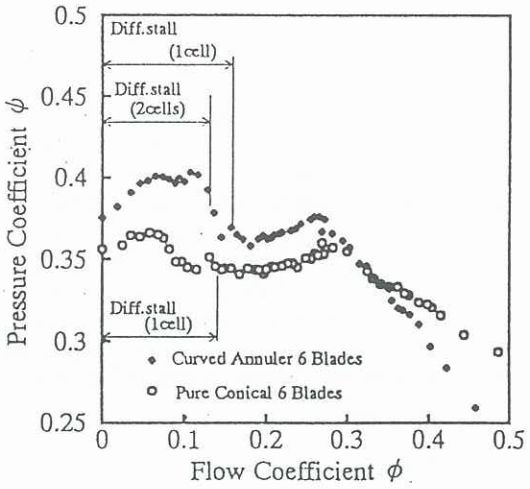

Fig.3 : Pressure coefficient vs. Flow coefficient

shown in Fig.3. The region of stable and unstable flow is clearly shown in the figures by the negative and positive gradient parts of the curves respectively. The range of rotating stall, detected by pressure transducers and hot wire anemometers, is also shown. The unstable zone, the positive sloping characteristic, is more clearly shown for the 12 bladed impeller than for the 6 bladed impeller, Fig.3, and rotating stall was not clearly detected when the 6 bladed impeller was used. The flow deviation from the blade direction at impeller discharge, the slip, will be greater for the 6 bladed impeller than for that with 12 blades. As a consequence the impeller discharge swirl will be less leading to a more radial flow through the vaneless diffuser and a reduced flow path length. This leads to reduced boundary layer growth and stall is less severe. Rotating stall caused by impeller stall and diffuser stall was clearly discernible by the rotational frequency. In this study, the frequency of impeller stall was approximately 70% of the impeller rotational frequency, while that for the diffuser was in the range 15% to 28%. The frequency of impeller and diffuser rotating stall, detected by the use of pressure transducers in the diffuser passage (R/R_2=1.275), is shown in Fig.4.

The detection of these rotating stall cells was also made by the measurement of velocity fluctuations, using a hot wire anemometer, at the impeller inlet. For the 12 bladed impeller, impeller rotating stall disappeared near the flow rate at which the minimum pressure coefficient occurred, see Fig.2. As the flow rate was reduced from this point, rotating stall caused by the diffuser appeared. Initially a single stall cell was detected but as the flow rate was further reduced two stall cells developed.

The different pressure characteristics of the machines, as shown in Fig.2 or Fig.3, is attributable to the alternative diffuser designs as both the upstream and downstream components are common, with the air discharging to the atmosphere in all cases. From the time averaged traverse measurements, Fig.5, it can be seen, for the pure conical diffuser, that as the flow rate is reduced the flow deviates towards the outer (shroud side) wall due to the swirl, and flow reversals develop on the inner wall (hub side) when the machine operates in the low

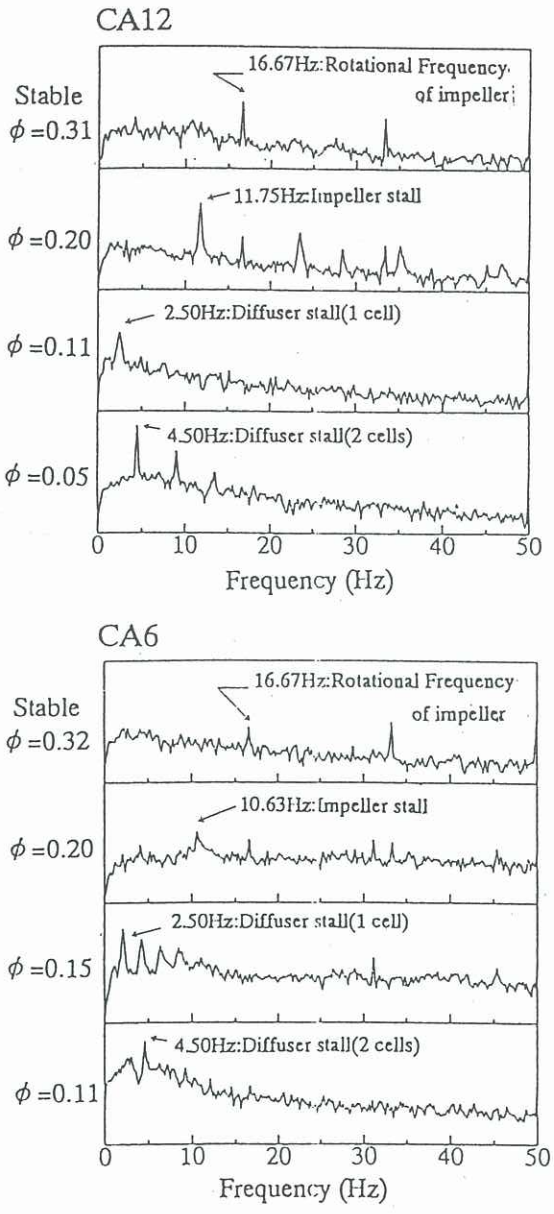

Fig.4 :Spectra of pressure fluctuation

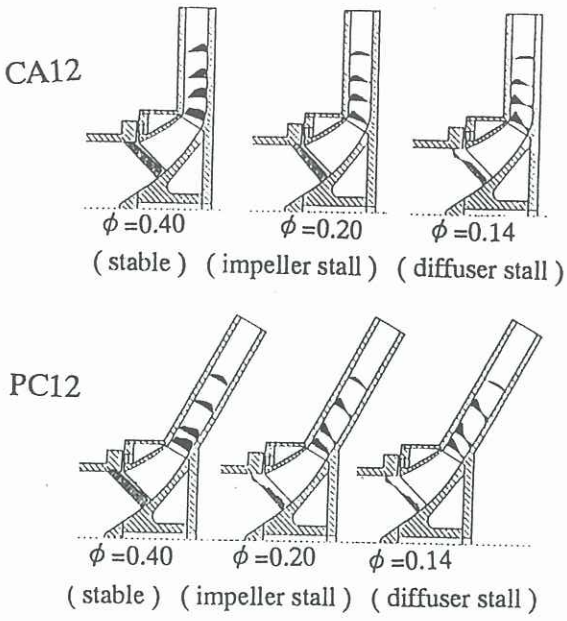

Fig.5 :Meridional velocity component

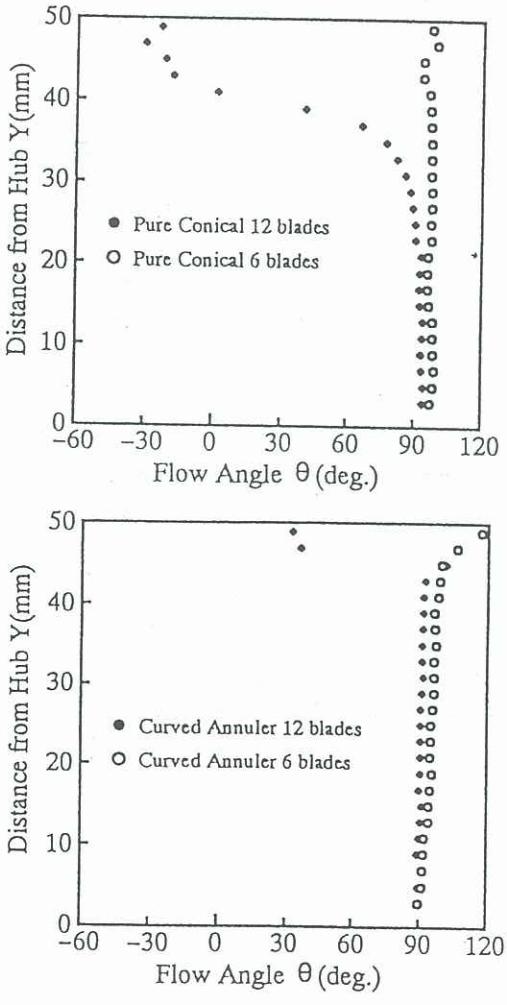

Fig.6 :Flow angle of the impeller inlet ϕ =0.20

flow region. Due to the blockage caused by the reverse flow on the hub side of the diffuser, the character of the flow in the impeller is changed as the discharge is forced towards the shroud side. For the curved annular diffuser the above mentioned blockage effect can also be seen at the flow rate at which rotating stall occurs, but the reverse flow region is reduced. From these diffuser flow measurements it can be seen that the inception of rotating stall occurs at higher flow coefficients with the pure conical diffuser than with the curved annular diffuser.

The flow conditions at impeller inlet were measured with a three hole cobra probe and the flow angle, for ϕ =0.2, is shown in Fig.6. Over much of the inlet passage from hub to shroud the inlet flow is axial and shows no swirl for all configurations tested. Substantial swirl and reverse flow in the shroud region of the 12 bladed impeller was observed when tested with the pure conical diffuser, the negative flow angles indicating reverse flow. With the curved annular diffuser the swirl flow at impeller shroud inlet is not as substantial nor dose it penetrate across the flow passage. Clearly the stall in the pure conical diffuser has effected the impeller inlet flow conditions. With the 6 bladed impeller the flow is uniform across most of the inlet passage when tested with both diffuser designs. Again this is possibly associated with the reduced swirl developed by the 6 bladed impeller leading to a shorter flow path through the vaneless diffuser and a reduced tendency to stall.

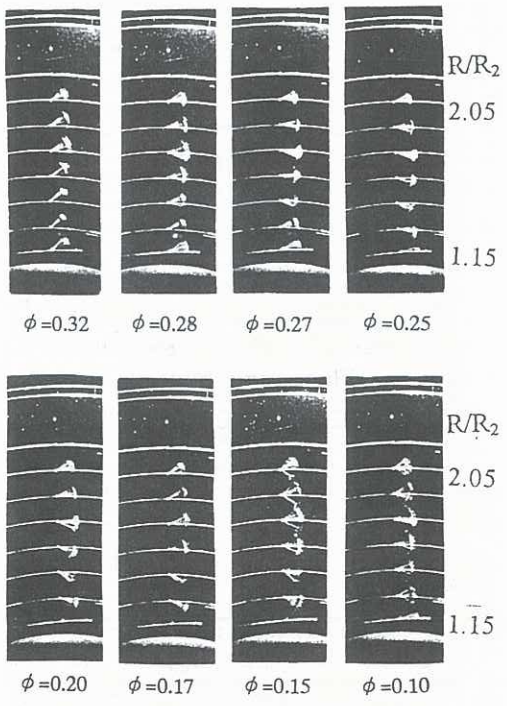

Fig.7 :Behaviour of tufts on diffuser hub wall (curved annular diffuser with 12 bladed impeller)

Fig.7 shows the pictures of the motion of the tufts attached on the hub surface of the curved annular diffuser when tested with the 12 bladed impeller as the flow rate was reduced. From the motion of these tufts it was observed that the reverse flow first commenced at the outer radius of the diffuser at a flow coefficient of 0.28. As the flow rate was reduced the reverse flow region moved towards the impeller discharge and the fluctuations became move violent; becoming most severe when diffuser rotating stall was established.

Fig.8 shows the pictures of tufts attached to the blade suction surface of the impeller with 12 blades. At the inception of rotating stall in the impeller, ϕ =0.27, large fluctuating motion of the tufts was observed near the shroud side. With reduction of the flow rate to ϕ =0.20 the tufts near the hub side also showed large fluctuations.

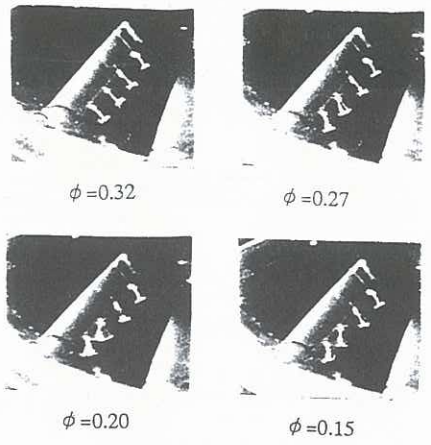

Fig.8 :Behaviour of tufts on suction surface of impeller inlet (12 bladed impeller)

Conclusions

1 The adoption of a pure conical diffuser design leads to the commencement of rotating stall at higher flow coefficients than when the diffuser is curved into the radial plane.

2 Flow deviation in impeller passage as well as the inception of impeller rotating stall is effected by flow reversals in the diffuser.

3 Diffuser rotating stall commences when the reverse flow on the hub wall, which originates at the outer radius of the diffuser, shifts towards the diffuser inlet/impeller exit.

4 Impeller rotating stall was not as clearly detected with the 6 bladed impeller compared with that for the 12 bladed impeller.

References

Abir, A., Whitfield, A., 1987, "Stability of Conical and Curved Annular Diffusers for Mixed-Flow Compressors," ASME paper 87-GT-191.

Sakai, T., Tezuka, K., Ito, N., Sakuma, H., Nizeki, Y., 1994, "Visualization of the Rotating Stall in a Mixed-flow Turbomachine," Proc. FLUCOME, Vol.2 pp679-684 1994.